SUNTEXT REVIEWS

SunText Review of Virology
ISSN: 2766-5003

Open Access
Research Article
Volume 1:1

Research on the Design and Control Strategy of Chang'e-3 Soft Landing Orbit and Its Sensitivity Analysis during the Epidemic of Coronavirus Disease

Li Y[1], Zhao H[1], Wang B[2], Zhu T[2], Wang Z[1], Li M[3] and Zhao B[1,*]

[1]*School of Science, Hubei University of Technology, Wuhan, Hubei, China*
[2]*School of Electrical and Electronic Engineering, Hubei University of Technology, Wuhan, Hubei, China*
[3]*Normal School of Vocational and Technical Education, Hubei University of Technology, Wuhan, Hubei, China*

[*]**Corresponding author:** Zhao B, School of Science, Hubei University of Technology, Wuhan, Hubei, China; Tel: +86 130 2851 7572; E-mail: zhaobin835 [at] nwsuaf (dot) edu (dot) cn

Received date: 24 June 2020; **Accepted date:** 07 July 2020; **Published date:** 12 July 2020

Citation: Li Y, Zhao H, Wang B, Zhu T, Wang Z, Li M, et al. (2020). Research on the Design and Control Strategy of Chang'e-3 Soft Landing Orbit and Its Sensitivity Analysis during the Epidemic of Coronavirus Disease. SunText Rev Virol 1(1): 101.

DOI: https://doi.org/10.51737/2766-5003.2020.001

Abstract

Aiming at the control strategy of the Chang'e-3 lunar landing, this paper establishes a single-target optimization model based on the variable dynamic Newton differential equation, uses iterative method to obtain the time discrete model, and uses the genetic algorithm based on double-precision real-number coding to obtain the variable dynamic parameters. The control strategy of each stage is given according to the constraint conditions of the six stages and the actual situation during the epidemic of Coronavirus Disease in China. The error propagation law is used to analyse the systematic deviation of the key parameters of the Chang'e-3, such as the velocity near the moon and the flight time. The Sobol method based on the Monte Carlo sampling method is used to analyse the global sensitivity of the two-body dynamic model by using the total order effect of the Sabol method.

In response to Question One, according to Kepler's third law and the law of universal gravity, the speed size of the near moon point and the distant moon point are 1692.7km/s and 1614.4m/s. Based on the dynamic differential equation of variable force, a single-target optimization model is established with the minimum fuel consumption as the constraint target. Using iterative method to separate time, the angle of thrust size, thrust direction and velocity in the opposite direction is encoded in real number, the range of the angle in the motion is 5.8°- 7.6° , the thrust size is 7500 N, and the horizontal is obtained in the inverse equation. Determined by the definition of longitude and latitude of the lunar heart coordinate system(19.51W,31.38N). In response to Question Two, a single/multiple objective optimization model is constructed based on the discrete dynamics equation of Question One and the optimization objectives and constraints in six stages. In the main deceleration stage, the target is the minimum deceleration time and the minimum fuel consumption, and weights of 0.6 and 0.4 are given, respectively. The genetic algorithm is used to solve the problem to obtain that this stage takes 416s, consumes 1062.1kg of fuel and has a final speed of 57m/s. The goal of the rapid adjustment stage is to minimize fuel consumption, which takes 257.7s and consumes 41.98kg of fuel. The final speed is 0.189m/s. Coarse obstacle avoidance phase Sobel operator is used to calculate the attachment image digital elevation map the gradient of the S(x, y) using median filter method to many times to deal with the noise of the gradient map, by the meshing method elevation graph corresponding to the demonising of gradient graph can be divided into 9 regions, with fuel consumption optimal, the optimal flatness as the optimization goal to determine the best mobile strategy for the regional centre moved to the left of 44 pixels. The rough obstacle avoidance stage took 133s, consumed 91.98kg of fuel, and the final speed was 0.5401m/s. In the fine obstacle avoidance stage, the same processing method was adopted as in the rough obstacle avoidance stage, and the optimal landing location was obtained as grid (4,6), moving to the upper right for 14m. The precise obstacle avoidance stage takes 97.8s, consumes 63.38kg of fuel, and the final speed is 0.1554m/s. In the slow descent

stage, variable force linear descent strategy was adopted. The thrust increased gradually from 1903N to 1908N, which took 68.8s and consumed 42.57kg of fuel. In the free fall stage, the final velocity before landing is 3.6051m/s and the final mass is 1097.8kg. In response to Question Three, the relative error expressions of velocity, flight time and horizontal displacement of Chang'e-3 near the moon point are solved by using the error propagation law, and the influence of system deviations of key parameters on the model error is calculated. The Sobol' method based on the Monte Carlo sampling method was used to analyse the global sensitivity of the two-body dynamics model by using the Sobol' total order effect. The first two main sensitivity factors of the global sensitivity analysis were obtained as the velocity variation and the main pushing force, and the sensitivity coefficients of the total order were 38.2515 and 37.8504 respectively.

Keywords: Chang'e-3 lunar probe; Two-Body dynamics model; Optimal control; Sobel operator; Real number coding genetic algorithm

Introduction

Background of the problem

The optimization design of the landing orbit and control strategy of The Chang'e-3 is the key to ensure that it can accurately achieve soft landing in the intended area of the moon under high-speed flight, and many researchers have divided the soft landing of the moon into brake segments, close segments and landing segments, and optimized the guidance of each stage. Optimized the guidance of the three stages of soft landing on the moon based on dynamic model, and made a preliminary simulation analysis of the landing accuracy [1]. The control scheme by combining nonlinear variable structure control with state feedback, and used Simulink software to simulate the resulting mathematical model and obtain satisfactory simulation results [2]. Uniform three-dimensional dynamics model of the moon's soft landing brake segment to obtain a fuel suboptimal guidance law, and studied the three-stage descent Trajectory and guidance law respectively [3]. Now, the moon soft landing process is divided into the main deceleration, rapid adjustment, coarse barrier avoidance, fine barrier avoidance, slow descent, free fall a total of 6 stages, and according to the requirements of each stage state to optimize the design of the landing orbit and control strategy to be studied, this paper takes the optimal fuel consumption in the soft landing process as the main design index, the soft landing of the Chang'e-3 as a six-stage after the landing orbit and control strategy design problems to be studied.

Related information

The data used in this paper is derived from the 2014 National University Mathematics Modelling Competition [4-6]. This question gives basic information on Change-3, which was successfully launched at 1:30 p.m. on December 2, 2013 and arrived in lunar orbit on December 6, 2013. The main deceleration engine installed in the lower part of the Chang'e-3 on the landing preparation track is 2.4t, and its main deceleration engine installed in the lower part can produce an adjustable thrust of 1500N to 7500N, which is 2940m/s of the thrust generated by the propellant of unit mass, which can meet the control requirements of the adjustment speed. The attitude-adjusted engine is installed around and the adjustment control of various attitudes can be automatically achieved by the pulse combination of multiple engines after a given thrust direction of the main deceleration engine. The scheduled landing point of Chang'e-3 is 19.51W, 44.12N and at an altitude of -2641m (see Annex 1). In addition, the six stages of the soft landing process (Annex 2) and the digital elevation map at 2400m and 100m on the lunar surface of the third is given in this question (Annex 3, 4).

Issues to be addressed

The basic requirements of the design of the landing orbit of Chang'e-3 are: 15km of the landing preparation orbit and 100km of the elliptical orbit of the far moon point, and the landing orbit is from the near-moon point to the landing point, and its soft landing process is divided into six stages, which requires the requirement of meeting the state of each stage at the critical point, and minimizing the fuel consumption of the soft landing process [7,8]. Based on the above basic requirements, a mathematical model is established to solve the following problems:

1. Determine the location of the near-moon and distant moon points in the landing preparation orbit, as well as the size and direction of the corresponding speed of the Chang'e-3.
2. Determine the landing orbit of Chang'e-3 and the optimal control strategy in six stages.
3. The corresponding error analysis and sensitivity analysis are made on the designed landing orbit and control strategy.

Problem Analysis

Regarding the soft landing of Chang'e-3 as six stages, considering the process of establishing a flat right-angle coordinate system with the moon's heart as the origin, considering the design of the various stages and control strategies of the landing orbit, and the specific analysis of the three questions in this question is as follows [9,10]:

Analysis of question one

Question one requires determining the speed and position of the Chang'e-3 at the near-moon point. In view of the determination of the near-moon point speed problem, because the distance between the near-moon point、the distant moon point and the lunar surface is known at this time, the other physical parameters of the moon are provided by Annex 1, the speed of the near-moon point and the distant moon point can be solved by the laws of mechanics and the law [11]. In order to determine the position of the near-moon point and the distant moon point, in the process, the motion state of the Chang'e-3 is unknown, it is difficult to establish a model describing the whole motion process to get the position directly, and it is necessary to establish a sports model that describes the amount of the process. Considering that the moon's lunar heart coordinate system can describe the latitude and longitude of any point on the moon, the use of the lunar centre coordinate system will simplify the description and resolution of the problem. On this basis, we also need to consider how to describe the relationship between the horizontal displacement and vertical displacement and longitude and latitude of the Chang's 3, and how to convert the relationship between them needs to be considered according to the actual situation. The approximate motion process can be judged according to the state at the end, combined with the initial state and the approximate shape of the entire motion process, and the specific amount of process needs to be further model to determine.

Analysis of question two

Question Two needs to determine the soft landing orbit of the Chang'e-3 and give the optimal control strategy of six stages. The optimal fuel consumption in the soft landing process should be regarded as the target of the six-stage control strategy and the landing orbit design, from the position of the near-moon point under the plane right-angle coordinate system and the speed at the near-moon point when the Chang'e-3 is ready to land, that is, the initial state of the Chang'e-3 in the main deceleration phase, Annex 2 gives the initial conditions of the Chang'e-3 speed and main engine thrust in the rapid adjustment to slow descent stage, and considering that the soft landing process can be regarded as a two-body problem, and always only the moon's gravity, engine thrust act on the Chang'e-3, it can be considered that the dynamic model established by the problem is general, so the initial conditions, constraints and dynamics of each stage are connected, can be in the centre-plane right-angle coordinate system to solve the optimal fuel consumption optimization model, so as to determine the optimal parameters of each stage and give the soft landing orbit and the optimal control strategy of each stage [12]. In addition, the continued decline of the Chang'e-3 after the requirement of the best landing site after the height map of the rough barrier and the fine barrier avoidance phase is determined by the two-goal optimization of fuel consumption and ground level to determine the optimal landing point and continue to decline [13,14]. Consider ingesting the image and using the Sobol operator to get the corresponding gradient map, to select the landing area, the image can be divided into 9 areas to select the optimal area.

Analysis of question three

Question Three requires error analysis and sensitivity analysis of the established model. In the two-body dynamics optimization model established for the soft landing process of the Chang'e-3, the key parameters such as the speed size of the near-moon point and the overall mass of the Chang'e-3 contain systematic deviations, the functions of flight time, horizontal displacement and so on about these key parameters are affected by it and also contain errors. Consider solving the partial differentials of the key parameters of the model, such as flight time and horizontal displacement, and substitute the known data such as boundary constraints of each stage into the partial differential expression to obtain the multi-equation equation, so as to determine the main error term that affects the target function. For sensitivity analysis, the first-order sensitivity coefficient and the overall level sensitivity coefficient of the key parameters of the model are solved by using the Sobol sensitivity analysis method based on Monte Carlo sampling method [15,16].

Question Assumptions

In order to reduce the complexity of this problem and simplify the establishment and solving of the model, the following basic assumptions are made before the model is established:

1. Suppose the landing preparation orbit is on the same plane as the moon orbit;
2. Suppose that the curvature of the moon has a negligible effect on the soft landing process;
3. Suppose the effects of the non-inertial coordinate system are negligible during soft landing;
4. Suppose that the Chang'e-3 and the Moon can be considered as two-body problems during a soft landing;

Note: The rationality analysis of the above basic assumptions can be found in the scenario analysis.

Symbol Description

To make the introduction to the model clear, this paper defines some of the symbols.

Note: Other symbols are specified in the text.

Model Building and Solving

This chapter establishes an optimization model, uses iterative method discrete dynamic differential equations, and uses genetic algorithms to solve the expressions of key unknown parameters.

Section 5.1 establishes the speed and position model of the near-moon and distant moon points, and section 5.2 establishes the two-body dynamics optimization model, and solves the control strategy and track parameters of each stage with the six-stage constraints. Section 5.3 analyses the error of the model by the law of error propagation, and the global sensitivity analysis of the model is analysed based on the Sobol total order effect.

The establishment and solution of the problem-one model

Based on Kepler's third law and energy conservation law, this section establishes a general model of the two-body problem to solve the speed size and direction of the near-moon and distant moon points, and establishes the dynamic differential equation of the Chang'e-3, with the minimum fuel consumption as the goal and the speed and position altogether as a constraint, and uses the Longekutta method to obtain the displacement of the Chang'e-3. The position of the near-moon point is solved according to the relationship.

Scene analysis

Analysis of the physical environment of the Chang'e-3 satellite and the corresponding numerical calculation, based on the results of analysis and calculation, the basic assumptions conducive to model analysis and solution, in the general situation, the problem is reasonably simplified.

Moon-Satellite system

During the Chang'e-3 lunar landing, it is not only influenced by the gravity of the moon and the thrust of the engine, but also influenced by the gravity of the earth and other celestial bodies, according to the law of universal gravitation [4].

$$F_1 = F_2 = \frac{GM_1M_2}{r^2}$$

Since the Earth-Moon distance is much larger than the Earth-Satellite distance, r of the formula can be replaced by the Earth-Moon distance $r = 3.844 \times 10^8 m, M_1 = 5.965 \times 10^{24} Kg$ is the mass of the earth,$M_2 = 2.4 \times 10^3 Kg$ is the mass of the satellite, the average force of the satellite by the Earth is calculated$F_1 = 6.464N$, and the average force of the moon to the satellite is obtained.

$$F \approx g_{moon}M_2 = 3.84 \times 10^3 N$$

Comparing the size of F and F_1, the Earth's force on the Chang'e-3 is negligible at the moon's gravity scale, as is the force of other celestial bodies on the Chang'e-3 [17]. Thus, a reasonable simplification can be made: when the dynamic analysis of the Chang'e-3 is carried out, only the lunar force and its own thrust, the moon and the Chang'e-3 can be regarded as a two-body system.

Landing readiness orbit and soft landing orbit with plane hypothesis

Considering the least fuel consumption, if the landing preparation orbit is not in the same plane as the soft landing orbit, the initial speed is reduced to 0 while consuming fuel to de-orbit the Chang'e-3 satellite. According to the law of energy conservation, the energy consumed by the Chang'e-3 is

$$E = \frac{1}{2}mv_1^2 + E_0$$

In the upper formula, E_0 is due to the energy required to deviate from orbit, so it is reasonable to treat the landing preparation orbit and soft landing orbit as the same plane in orbit design, without losing generality, and it can be assumed that the lunar rotation axis is also on the "dual orbit" plane. In fact, both the Chang'e-1 and the Chang'e-2 are designed as polar satellites [18]. Which also means that this assumption is reasonable in the optimization of the design and control strategy of the lunar orbit of the Chang'e-3 (Figure 1).

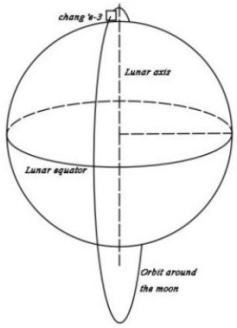

Figure 1: *A map of the same plane as the satellite "dual orbit" and the moon's spin axis.*

Solution of the velocity of the near-moon point

Chang'e-3 is affected by the moon's gravity in elliptical orbit, at this time the model of the two-body system composed of the moon and the moon is shown in (Figure 2), using Kepler's third law and energy conservation law can solve the near-moon point and the distant moon point of the Chang'e-3 in the elliptical orbit of the moon [19].

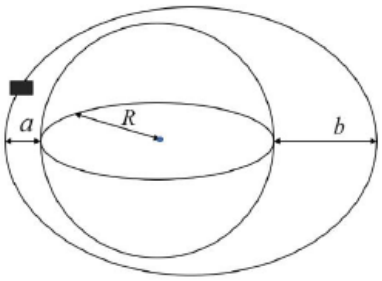

Figure 2: *Map of the Moon's two-body system.*

During the movement of the Chang'e-3 satellite, when the Chang'e-3 moves between the near-moon point and the distant moon point, the sum of its potential and kinetic energy remains the same, i.e. the mechanical energy is always subsertic.

$$\frac{1}{2}mv_a^2 - \frac{GMm}{R_a} = \frac{1}{2}mv_b^2 - \frac{GMm}{R_b} \qquad (1)$$

In the upper formula, v_a is the speed size of the Chang'e-3 at the near-moon point, v_b is the speed size at the distant-moon point, m is the mass of the Chang'e-3 satellite, the size is 2400kg, M is the mass of the moon, the size is $7.3477 \times 10^{22} Kg, R_a, R_b$ is the half-long axis and half-short of the elliptical orbit where the near-moon point and the distant-moon point are located.

The relationship between the near moon point, the distant moon point and the moon in the elliptical orbit of Figure 2 shows that the distance between the near moon point and the distant moon point from the centre of the moon is$R_a = R + a, R_b = R + b,$ (2)

Where, R is the mean radius of the moon, and$a$, b are 15km and 100km respectively. According to Kepler's third law, the satellite sweeps the same area in the same time, thus the following equation can be obtained

$$\frac{1}{2}v_a R_a = \frac{1}{2}v_b R_b \qquad (3)$$

Thus, the joint (1), (2), (3) can be obtained

$$\begin{cases} v_a^2 = \dfrac{2GMR_b}{(R_a + R_b)R_a} \\ v_b^2 = \dfrac{2GMR_a}{(R_a + R_b)R_b} \end{cases}$$

According to

$$M = 7.3477 \times 10^{22} Kg, G = 6.672 \times 10^{-11} N.\frac{m^2}{Kg^2}, R_a = 1752013m, R_b = 1837013m,$$

The speed size of the Chang'e-3 at the near-moon point and the distant-moon point can be solved.

V_a=1692.7m/s, $V_b = 1614.4m/s,$

According to the plane diagram of landing preparation orbit, moon landing orbit and moon rotation axis shown in Figure 1, the velocity direction of Chang'e-3 at the near and far moon points is perpendicular to the moon's gravity and coincides with the plane of the elliptical orbit.

Near-moon and distant-moon locations

The establishment of flight dynamics optimization model: Analysis of the scene, the landing preparation orbit of the Chang'e-3 is in the same plane as the soft landing orbit and coincides with the moon's rotation axis, and the topic requires the resolution of the location of the near and distant moon points and the intended landing point Longitude and latitude information, based on this, the three-dimensional scene shown in Figure 1 is transformed into the right-angle coordinate system of the moon's centre plane, and the dynamic analysis of the soft landing phase of the Chang'e-3 is followed by the reverse performance of the position information of the near-moon and distant moon points [20]. In the right-angle coordinate system of the moon's centre plane shown in (Figure 3), the origin O is the centre of the moon, with the direction of the near-moon point from the centre of the moon being x axis, the vertical direction being y axis, _ being the angle between the moon's gravity and the y -axis direction at some point in orbit, and (x, y) for the coordinates of the Chang'e-3 at the soft landing orbit somewhere, and Figure 3 also gives the analysis of the soft landing process of the Chang'e-3. In fact, the force state and change of the Chang'e-3 in the six stages are basically the same, without losing generality, this section in Figure 3 shows the moon centre plane right-angle coordinate system for the first force analysis and the establishment of a general dynamic model, for solving the near-moon and distant moon point positions.

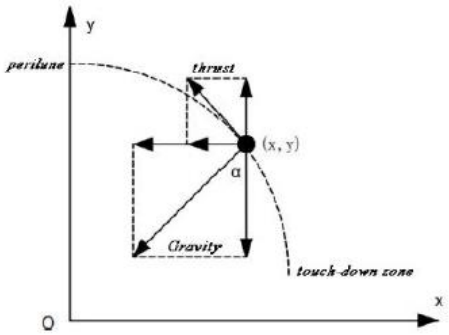

Figure 3: *Diagram of the right-angle coordinate system and force analysis of the heart plane of the month.*

During the soft landing, the engine thrust and the moon's gravity will change as the time and position of the landing orbit change [21]. Assuming that in the nth stage of the soft landing process, the main engine thrust $u_n(t)$ is $u_{xn}(t)$ and $u_{yn}(t)$ in the direction of x and y axes, and the angle between the gravity of the moon and the direction of the y axis is $\propto_n (t)$, and the motion equation of the Chang'e-3 can be established as follows

$$\frac{d^2x_n}{dt^2} = \frac{GM_M}{x_n^2+y_n^2} sin \propto_n (t) + \frac{u_{xn}(t)}{m_n(t)},$$
$$\frac{d^2Y_n}{dt^2} = \frac{GM_M}{x_n^2+y_n^2} cos \propto_n (t) + \frac{u_{yn}(t)}{m_n(t)}.$$

Of these, n =1, 2, 3, 4, 5, 6. Indicates that the Chang'e-3 is in the nth stage of the soft landing process. In addition, during the soft landing, the main thrust direction and the speed direction of the Chang'e-3 may become some kind of functional relationship, remember that the main engine thrust and speed in the opposite direction of the angle of $\theta_n(t)$, according to Figure 3 shows the relationship between the right-angle coordinate system of the moon's centre plane, it can be seen

$$tan \propto_n (t) = \frac{x_n(t)}{y_n(t)},$$
$$u_n(t).cos\big(\alpha_n(t) - \theta_n(t)\big) = u_{xn}(t),$$

$$u_n(t).sin\big(\alpha_n(t) - \theta_n(t)\big) = u_{yn}(t),$$

Among them, $x_n(t), y_n(t)$ are the coordinate values of the position of the t[th] stage of the moment, the position of the Chang'e-3 in the soft landing orbit, as can be seen by the definition of the main engine ratio punch

$$\frac{dm}{dt} = \sqrt{\frac{u_{xn}^2(t) + u_{yn}^2(t)}{v_e}}$$

Among them, v_e is the main engine ratio punch. During soft landing, optimal fuel consumption is always the goal of optimal control, i.e.

$$\text{Min}z = \int_{t_0}^{t_{final}} \frac{\sqrt{u_{xn}^2(t)+u_{yn}^2(t)}}{v_e} dt.$$

Taking into account the boundary constraints and process constraints of the various stages of the soft landing process, a general optimization model can be established as follows:

$$\text{Min}z = \int_{t_0}^{t_{final}} \frac{\sqrt{u_{xn}^2(t)+u_{yn}^2(t)}}{v_e} dt.$$

$$s.t\begin{cases} \frac{d^2x_n}{dt^2} = \frac{GM_M}{x_n^2+y_n^2} sin\propto_n(t) + \frac{u_{xn}(t)}{m_n(t)} \\ \frac{d^2Y_n}{dt^2} = \frac{GM_M}{x_n^2+y_n^2} cos\propto_n(t) + \frac{u_{yn}(t)}{m_n(t)} \\ \frac{dm}{dt} = \frac{\sqrt{u_{xn}^2(t)+u_{yn}^2(t)}}{v_e}, \\ m(t_0)=m_0, x_n(t_0)=x_0, y_n(t_0)=y_0, \frac{dx_n}{dt}(t_0)=\frac{dy_n}{dt}(t_0)=v_{y_0} \\ m(t_{final})=m_{final}, x_n(t_{final})=x_{final}, y_n(t_{final})=y_{final}, \frac{dx_n}{dt}(t_{final})=\frac{dy_n}{dt}(t_{final})=v_{y_{final}} \end{cases}$$

(4)

Where, $n = 1, 2, 3, 4, 5, 6.$ represents the nth stage of the soft landing process, and the equation (4) has a geometric relationship in the established centre plane right-angle coordinate system as follows

$$\begin{cases} tan \propto_n (t) = \frac{x_n(t)}{y_n(t)}, \\ u_n(t).cos\big(\alpha_n(t) - \theta_n(t)\big) = u_{xn}(t), \\ u_n(t).sin\big(\alpha_n(t) - \theta_n(t)\big) = u_{yn}(t), \end{cases}$$

According to the equation (4), it can be seen that the optimal orbital design and control strategy of the Chang'e-3 in different stages of the soft landing process is basically the same in each stage, mainly the initial state and termination state of the corresponding stage, that is, there are differences in the boundary constraints, which need to be discussed in stages. The establishment of the position model of the near-moon point and the distant moon point. The main role of the Chang'e-3 in the main deceleration segment is relatively long, the main role of this stage should be understood as eliminating the large initial horizontal velocity of the Chang'e-3 leaving the elliptical orbit and entering the soft landing orbit, and the optimal track design and control strategy for solving the optimal track design and control strategy for the main slow segment with the optimal fuel consumption optimization is the top priority of the overall soft landing process [22].

The general dynamic optimization model of the established Chang'e-3 when flying in the landing orbit, i.e. formula (4), can solve the optimal orbit design and control strategy for the main deceleration segment, and use the information of the pre-determined landing point latitude and longitude to reverse the position of the near-moon and distant moon point in turn. For the solution of the optimal track design and control strategy of the main deceleration segment, the optimization target, the two-body dynamics model and the constraints are established in turn as follows:

Optimize the target and two-body dynamics model

$$\text{Min } Z = \int_{t_0}^{t_{f1}} \frac{\sqrt{u_{x1}^2(t)+u_{y1}^2(t)}}{v_e} dt.$$

$$\begin{cases} tan \propto_1 (t) = \frac{x_1(t)}{y_1(t)} \\ u_1(t).cos\big(\alpha_1(t) - \theta_1(t)\big) = u_{x1}(t), \\ u_1(t).sin\big(\alpha_1(t) - \theta_1(t)\big) = u_{y1}(t), \\ \frac{d^2x_1}{dt^2} = \frac{GM_M}{x_1^2+y_1^2} sin \propto_1 (t) + \frac{u_{x1}(t)}{m(t)} \\ \frac{d^2Y_1}{dt^2} = \frac{GM_M}{x_1^2+y_1^2} cos \propto_n (t) + \frac{u_{y1}(t)}{m(t)} \\ \frac{dm}{dt} = \frac{\sqrt{u_{x1}^2(t)+u_{y1}^2(t)}}{v_e} \end{cases} \quad (5)$$

)

Among them, t_{f1} is the end of the main deceleration segment, the optimization target is the primary deceleration segment fuel consumption is minimal, v_e is still the main engine ratio, x, y is the position coordinate situ value of the corresponding flight time of the main deceleration segment, $\propto_1 (t)$ is the angle of the moon's gravity direction and the moon's plane right angle coordinates y axis, $u_{x1}(t)$ and $u_{y1}(t)$ are the main engine thrust in the x, y direction component size.

Constraints of the dynamic model of the main deceleration segment

The initial state of the main deceleration section is the state of Chang'e-3 at the near-moon point. According to its initial mass (unit: kg), position coordinate (unit: m) and initial velocity (unit: m/s), the initial constraint conditions are as follows

$$m(t_0) = 2400, x_1(t_0) = 0,\ y_1(t_0) = 1752013, \frac{dx_1}{dt}(t_0) = 1692.7, \frac{dy_1}{dt}(t_0) = 0 \quad (6)$$

According to the basic requirements of the main deceleration segment, it is known that the main gear segment ends with the following constraints on the position (unit: m) and the speed unit (m/s) as follows:

$$\sqrt{x_1^2(t_{f1}) + y_1^2(t_{f1})} = 1737373, \sqrt{\left(\frac{dx_1(t_{f1})}{dt}\right)^2 + \left(\frac{dy_1(t_{f1})}{dt}\right)^2} = 57. \quad (7)$$

Thus, after equations (5), (6) and (7) are combined, the two-body dynamics optimization model of the Chang'e-3 in the main deceleration section of the landing orbit is obtained as follows:

$$\text{Min } Z = \int_{t_0}^{t_{f1}} \frac{\sqrt{u_{x1}^2(t) + u_{y1}^2(t)}}{v_e} dt.$$

$$\begin{cases} tan \propto_1 (t) = \dfrac{x_1(t)}{y_1(t)} \\ u_1(t).cos(\alpha_1(t) - \theta_1(t)) = u_{x1}(t), \\ u_1(t).sin(\alpha_1(t) - \theta_1(t)) = u_{y1}(t), \\ \dfrac{d^2x_1}{dt^2} = \dfrac{GM_M}{x_1^2 + y_1^2} sin \propto_1 (t) + \dfrac{u_{x1}(t)}{m(t)}, \\ \dfrac{d^2y_1}{dt^2} = \dfrac{GM_M}{x_1^2 + y_1^2} cos \propto_1 (t) + \dfrac{u_{y1}(t)}{m(t)}, \\ \dfrac{dm}{dt} = \dfrac{\sqrt{u_{x1}^2(t) + u_{y1}^2(t)}}{v_e}, \\ m(t_0) = 2400, x_1(t_0) = 0,\ y_1(t_0) = 1752013, \dfrac{dx_1}{dt}(t_0) = 1692.7, \dfrac{dy_1}{dt}(t_0) = 0, \\ \sqrt{x_1^2(t_{f1}) + y_1^2(t_{f1})} = 1737373, \sqrt{\left(\dfrac{dx_1(t_{f1})}{dt}\right)^2 + \left(\dfrac{dy_1(t_{f1})}{dt}\right)^2} \end{cases}$$

Solution of the near-moon point and the distant-moon point location model

The formula (8) is a single-target nonlinear optimization model, the period solution is the optimal solution of infinite dimension, if the traditional optimization model solution method is difficult to get more correct solution quickly. In theory, the model must be able to solve the optimal motion trajectory and related parameters of the control strategy, consider the actual physical meaning of the model, the time discrete, the error allows for iterative solution of the model.

First of all, under the dynamic model with a large motion speed, the time is discrete, the time step is $\Delta t = 0.01$, consider that the motion state of the system can be regarded as the mean acceleration motion in a very short period of time, and the solution of the average acceleration motion model can be iterative solution, with the current time t state as the state within the next time period $(t, t + \Delta t)$, constantly update the speed and position, stop updating when the constraints are met, the iteration model is as follows.

$$\begin{cases} \left(x_{(t,t+\Delta t)}, y_{(t,t+\Delta t)}\right) = (x_t, y_t) + (\Delta x, \Delta y) \\ \left(v^x_{(t,t+\Delta t)} v^y_{(t,t+\Delta t)}\right) = \left(v_t^x, v_t^y\right) + \left(a_t^x \Delta x, a_t^y \Delta y\right) \end{cases}$$

Where, Δx is the horizontal displacement of the Chang'e-3 in Δt and Δy is the displacement of the Chang'e-3 in the vertical direction, which can be calculated by using Newton's second law in the application of uniformly accelerated motion

$$(\Delta x, \Delta y) = \left(\frac{\left(v^x_{(t,t+\Delta t)}\right)^2 - (v_t^x)^2}{2a_t^x}, \frac{\left(v^y_{(t,t+\Delta t)}\right)^2 - \left(v_t^y\right)^2}{2a_t^y} \right)$$

Where the horizontal direction speed and vertical direction speed can be determined by formula 3, there is by the acceleration of the formula 4

$$\begin{cases} a^x_{(t,t+\Delta t)} = a_t^x \\ a_t^x = \dfrac{GM}{x_t^2 + y_t^2} \dfrac{x_t}{(x_t^2 + y_t^2)^{1/2}} + \dfrac{F_t}{m(t)} cos\theta \end{cases}$$

The formula 5 can get the acceleration in the vertical component is

$$\begin{cases} a^y_{(t,t+\Delta t)} = a_t^y \\ a_t^y = \dfrac{GM}{x_t^2 + y_t^2} \dfrac{x_t}{(x_t^2 + y_t^2)^{1/2}} + \dfrac{F_t}{m(t)} sin\theta \end{cases}$$

And according to the initial conditions and constraints

$$\begin{cases} m_0 = 2400, \\ v_0^x = 1692.7, v_0^y = 0, \\ x_0 = 0, y_0 = 1752013, \\ s_{f1} = 1737373, v_{f1} = 57, \\ a_0^y = \dfrac{GM}{y_0^2} + \dfrac{F_0 sin\theta_0}{m_0}, \\ a_0^x = \dfrac{F_0 cos\theta_0}{m_0}. \end{cases}$$

The discrete numerical solution under the model can be obtained by iterative solution of the joint vertical 3, 4, 5, 6, 7. Considering that the angle of thrust and velocity in the opposite direction is unknown, it may be useful to set the angle and time t in the opposite direction of thrust and velocity to meet

$$\theta(t) = c_1 t^2 c_2 t + c_3$$

Where $c_k$an unknown coefficient, and the combination of time is obtains the angle size of the inverse direction of any time thrust and velocity. Considering the global optimal solution, this paper uses a genetic algorithm based on double-precision real-number coding to estimate the unknown parameter c_k and obtain the infinite dimensional optimal solution of the discrete iteration model.

The core idea of genetic algorithm based on double-precision real-number coding

Define the fitness function to describe the merits of the population, each individual in the population corresponds to an adaptation value, and retains the better individual sand and population for the operation of the adaptation value. Taking into account the cross-variation of nature, the individual in the population is cross-variation treatment, so as to meet the requirements of global optimality.

Step 1: The target items, such as the minimum fuel consumption and the constraints of speed and distance, are the empowerment values of the three, and the adaptability function is obtained, the smaller the adaptation value, the better the individual or population.

Step 2: Take 100 population iterations, each population set 50 individuals.

Step 3: Each individual is assigned within a reasonable solution range, and the numeric type is double-precision real.

Step 4: calculating the adaptation values of individuals preserves the less adaptable individuals as good individuals.

Step 5: Set the roulette wheel to carry out the individual variation cross and other operations, the probability of variation is 0.2, cross is 0.8

Step 6: After calculating the adaptive value after the variation, the population is constantly updated to obtain the unknown parameter value under the optimal population.

Based on the above algorithm, the adaptive value of the population with a population of 50 has stabilized after 35 iterations, and the global superior solution of parameter c_k is the

$$\begin{cases} c_1 = 1.1937 \times 10^{-5} \\ c_2 = 2.5681 \times 10^{-4} \\ c_3 = 5.7023 \end{cases}$$

When the angle between thrust direction and velocity direction satisfies the parameters in the above equation, the first two major corrections of the relationship type are corrected, and the final constant term is determined, and the angle of the angle is as shown in Figure 4 of the time change.

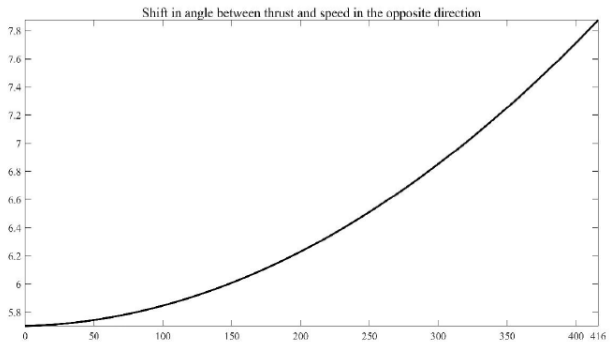

Figure 4: *Shift in angle between thrust and speed in the opposite direction.*

As shown in Figure 4, the angle between thrust and velocity in the opposite direction gradually increases with time, and the rate increases with increasing speed. The range of change is from 5.7° to 7.8°. If the initial Angle is not zero, it means that the attitude of the Chang'e-3 is in a certain angle with the velocity direction when it flies near the moon. If the angle becomes larger, it means that the attitude of the Chang'e-3 is constantly changing during the descent.

A graph of the angle θ generation in the iterative equation for the solution to obtain the angle changes over time the aircraft height, aircraft mass, aircraft velocity, and angle of thrust direction and velocity direction over time, as shown in Figure 5.

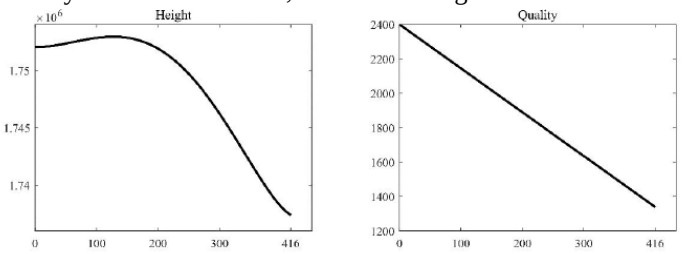

Figure 5: *Height and Quality Change Chart.*

As the height and mass and time changes in the map, the height of the main deceleration of the Chang'e-3 first rises and then drops, in fact, due to the relative to the moon coordinate system of the position change. The Chang'e-3 spent 416s during the main deceleration phase, dropping from 17542013m to 1737373m, with a horizontal displacement of 38306m. According to the longitude and latitude relationship of the lunar coordinate system, if the longitude value of the Chang'e-3 does not change significantly during the main deceleration phase, the change value of latitude can be expressed by horizontal displacement and the radius of the moon, as follows.

$$\Delta w = arcsin\frac{\Delta x}{R}$$

Δw Is the change value of latitude, and the radius of the moon is 1737013m, the horizontal displacement is 38306m, and the change value of latitude is 12.74°. The latitude and longitude of the landing point of the Chang'e-3 is (19.51W, 44.12N), and according to the direction of operation of the Chang'e-3 is from the south to the north of the moon, the latitude and longitude of the near-moon point can be obtained (19.51W, 31.38N), the near-moon point speed is 1692.7m/s.

The establishment and solution of the problem two model

The optimal fuel consumption is the optimization goal of the track design and control strategy through the six stages of soft landing on the Chang'e-3, and the optimization goal of the track design and control strategy is the optimal fuel consumption and floor

flatness in the stage of coarse barrier avoidance and fine obstacle avoidance [23]. Depending on the soft landing process as a two-body problem, the state requirements of each stage, that is, the initial conditions and other constraints of the speed of each stage and the thrust of the main engine, and the optimization model and solution method established by the dynamic differential equation system are combined with the initial conditions and other constraints of the main engine thrust respectively, and the flight speed, main engine thrust, thrust and speed angle of the stage of the Chang'e-3 is determined. The optimal orbit design and control strategy scheme for 6 stages of soft landing process are given. This section includes 5.2.1-5.2.6, with six subsections describing the main deceleration stage, the rapid adjustment stage, the coarse barrier avoidance stage, the fine barrier avoidance stage, the slow descent stage, the free-fall stage different solution models and results, each section ends to give the optimal motion trajectory and important parameters of the control strategy.

Optimal motion trajectory and control strategy for the main deceleration segment

The establishment and solution of the flight dynamics optimization model in the main deceleration stage of the Chang'e-3 has been given in 5.1.3, and the change curve of the key parameters of the main engine thrust direction, motion trajectory, running speed and other orbit design and control strategy is shown in Figure 6.

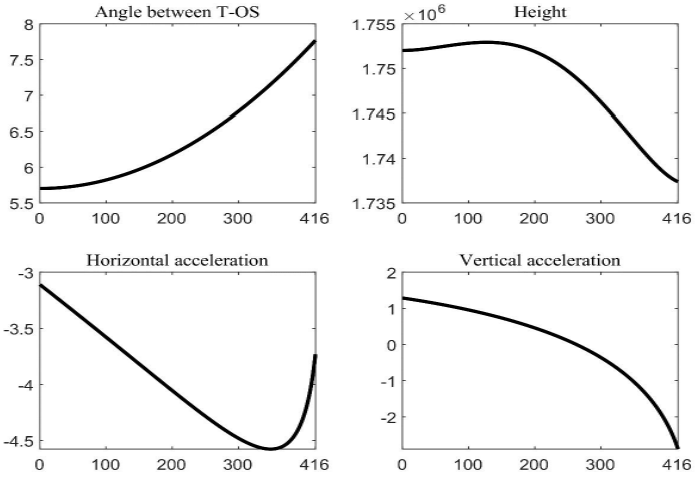

Figure 6: *Control parameters for optimal flight status.*

The angle of thrust direction and velocity in the opposite direction gradually increased, from 0°degrees to 7°or 8°, the height went through the process of first becoming large and then small, the horizontal acceleration showed the reverse hook type, reflecting the pattern of the horizontal acceleration increased and then decreased, and the vertical acceleration went through the process of steering. The main deceleration phase takes 416s, consumes 1062.1kg of fuel, has a residual mass of 1337.9kg, and the horizontal displacement is 38306m and the vertical displacement is 12km.

Rapid adjustment of the optimal motion trajectory and control strategy of the segment

During the soft landing of the Chang'e-3, the role of the rapid adjustment phase can be regarded as reducing the speed of the horizontal direction of the Chang'e-3 to 0 on the basis of the main deceleration phase, and the attitude of the Chang'e-3 can be adjusted rapidly, so that the thrust direction of the main engine and the gravitational direction received are basically in a straight line [24]. Considering the fast adjustment phase is relatively short time, so the optimal fuel consumption is not the main problem of this stage, and the final state of the fast adjustment phase will directly affect the image acquisition of the landing area surface condition in the stage of the rapid adjustment, it can be understood that the main role of the rapid adjustment phase should be understood as making the Chang'e-3 adjusted to the basic requirement state as soon as possible.

The establishment and solution of the rapid adjustment segment optimization model

During the rapid adjustment phase, the direction of the $u_2(t)$ main engine thrust needs to be gradually adjusted to the right-angle coordinate system of the moon centre plane y-axis positive half-axis direction, and in the process of falling 600m, the velocity of the horizontal direction (direction parallel to the x-axis of the right-angle coordinate system of the moon's centre plane) should be reduced to 0. For the solution of optimal track design and control strategy for rapid adjustment stage, the optimization target, the two-body dynamics model and the constraints are established in turn.

Optimising goals

The optimization goal of the track design and control strategy of the Chang'e-3 in the fast-adjustment phase is still to have the lowest fuel consumption, i.e.

$$\text{Min } Z = \int_{t_0}^{t_{f2}} \frac{\sqrt{u_{x2}^2(t)+u_{y2}^2(t)}}{v_e} dt. \qquad (9)$$

Where, t_{f2} is the end of the rapid adjustment phase, and the meaning of other symbols and general optimization models is consistent with the equation (4)

Two-body dynamics model

In the fast-adjustment phase, the Chang'e-3 is still only subject to engine thrust and the moon's gravitational effect on it.

$$\frac{d^2x_1}{dt^2} = \frac{GM_M}{x_2^2+y_2^2} sin \propto_2 (t) + \frac{u_{x2}(t)}{m(t)},$$

$$\frac{d^2y_2}{dt^2} = \frac{GM_M}{x_1^2 + y_1^2} cos \propto_2 (t) + \frac{u_{y2}(t)}{m(t)},$$

$$\frac{dm}{dt} = \frac{\sqrt{u_{x2}^2(t) + u_{y2}^2(t)}}{v_e}, \qquad (10)$$

$$u_2(t).cos\big(\alpha_2(t) - \theta_2(t)\big) = u_{x2}(t),$$

$$u_2(t).sin\big(\alpha_2(t) - \theta_2(t)\big) = u_{x2}(t),$$

Among them, $\alpha_2(t)$ is the angle between the gravity of the moon and the y axis direction of the rectangular coordinate system of the lunar centre plane, $\theta_2(t)$ is the angle between the thrust direction and the speed of the main engine, and the Chang'e-3 during the rapid adjustment phase $\alpha_2(t)$ and $\theta_2(t)$ will continue to change, its two-body dynamics model equation (10) is consistent with the main deceleration section.

Boundary constraints

The initial state of the Chang'e-3 during the rapid adjustment phase of the soft landing process can be regarded as its state at the end of the main deceleration stage. The results of the optimization model of the main deceleration stage and the attachment information can list the quality of the Chang'e-3 during the rapid adjustment stage the boundary constraints of (unit: kg), position coordinates (unit: m) and flight speed (unit: m / s) are as follows:

$m_2(t_0) = 1341.33, x_2(t_0) = 380219.57,\ y_2(t_0) = 1695251.32, \frac{dx_2(t_0)}{dt} = 39.64, \frac{dy_2(t_0)}{dt} = -40.96,\ \sqrt{x_2^2} = 1736773, \sqrt{\left(\frac{dx_2(t_{f2})}{dt}\right)^2 + \left(\frac{dy_2(t_{f2})}{dt}\right)^2} = 0 \qquad (11)$

At this point, the above equations (9), (10), (11) were established to establish the Chang'e-3 track design and control strategy optimization model during the rapid adjustment phase.

Solution and analysis of the model in the stage of rapid adjustment

First difference iterative optimization model can be converted to same format, using the improved real-coded genetic algorithm for $\theta_2(t)$ expression of unknown parameters for the optimal solution, to determine the optimal parameters after the substitution difference iterative format, in the case of allowable error solving fast adjustment phase optimization model of numerical optimal solution, using the MATLAB software to quick adjustment period to solve optimization model. Through the improved real-coded genetic algorithm, the thrust size of the main engine, the thrust direction of the main engine and the angle of the reverse angle between the speed and the thrust direction of the main engine $\theta_2(t)$ in the rapid adjustment phase were solved, and the constant thrust of the main engine in the rapid adjustment phase was 4791.3N, while the relationship between $\theta_2(t)$ and the time t of the Chang'e-3 in the rapid adjustment phase was satisfied

$\theta_2(t) = 1.3672 \times 10^{-4}t^2 + 6.7078 \times 10^{-4}t + 1.1652 \qquad (12)$

The equation (12) generation into the differential iteration format to solve the optimization model, the horizontal direction speed size of the third at the end of the fast adjustment phase is 0.0098m/s, vertical direction speed size is 0.1807m/s, in the optimal fuel consumption in the rapid adjustment stage is 41.98kg, the overall residual mass of the Chang'e-3 is 1295.9kg, and the total time-consuming time of the rapid adjustment phase is 25.9s. The optimal motion trajectory and parameter control of the fast adjustment stage of the Chang'e-3 is shown in Figure 7.

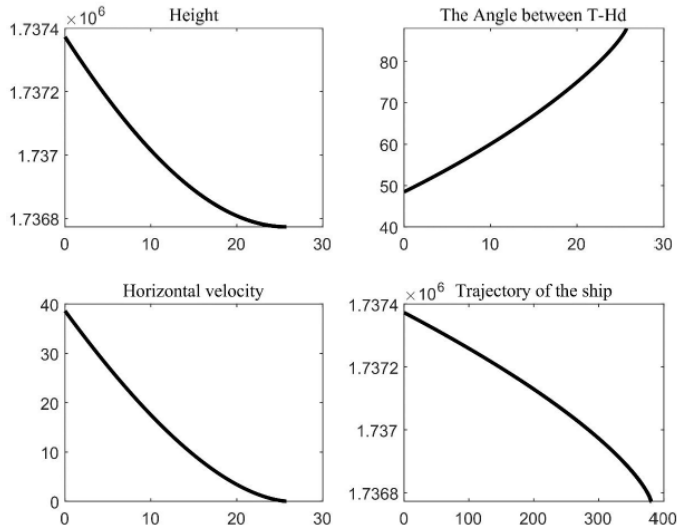

Figure 7: *Quick adjustment of segment motion trajectory and parameter control schematic.*

In Figure 7, the upper left image is a schematic of the change of the height of the Chang'e-3 in the fast-adjustment phase over time, the horizontal axis is the time (units), the vertical axis is the height (unit: m), and the upper right image is a diagram of the time-change angle between the main engine thrust and the vertical direction, and it can be seen that in the 25.9s of the rapid adjustment phase, the main engine thrust and horizontal angle change gradually from 50° to 90° . gradually increase; In this stage, the horizontal velocity of the Chang'e-3 will also be reduced to 0m/s in a state where the rate of change is gradually decreasing, and the lower right image is the optimal motion trajectory of the rapid adjustment phase, the horizontal axis of the graph is the horizontal displacement, the vertical axis represents the vertical shift, it is worth noting that the horizontal displacement of 44m relative to the vertical displacement of 2300m is small, which can be regarded as the trajectory of the movement of the Chang'e-3 as a straight line in the rapid adjustment phase (Table 1).

Table 1: *Explanation of Symbols.*

Symbol	Describe	Unit
M_M	The mass of the moon	kg
r_M	The distance between the third and the heart of the moon	m
g_M	The moon's gravitational acceleration to the Chang'e-3	kg/s^2
V_A	The speed of the Chang'e-3 in the near-moon	m/s
t	The time when the Chang'e-3 fell in the landing orbit	s
$u_n(t)$	Thrust of the main engine in stage *n*	N
$\theta_n(t)$	Angle between the thrust and speed of the main engine stage n	°
V_B	The speed of the Chang'e-3 at the distant moon point	m/s
$\propto_n (t)$	Stage *n* gravity and moon-center plane right-angle coordinate system y-axis angle	°

The establishment and solution of the rough barrier segment model

The initial state of the Chang'e-3 in the rough barrier phase can be understood as the end state of the rapid adjustment phase, according to the solution results of the rapid adjustment segment optimization model, the position coordinates (unit: m) at the end of the fast adjustment phase under the right-angle coordinate system of the moon's heart plane are (380653. 334,1694558.626), the flight speed (unit: m/s) on the x、y axes components 0.214 m/s, -0.573m/s , mass of 1297.675 kg. The role of the coarse barrier avoidance phase should be understood as determining the optimal landing position and determining the control strategy of the main engine to move the Chang'e-3 to the optimal landing site. Establishment and solution of the optimal landing point model of rough barrier avoidance segment.

This section uses Sobel operator to calculate the gradient S(x, y) of the digital elevation map of the attachment image, and uses the median filtering method to perform multiple denoise processing on the gradient map, and after dividing the denoise gradient map corresponding to the elevation map into multiple regions by meshing, the optimal fuel consumption and flatness are optimized to determine the optimal landing point [25].

Image processing for digital elevation diagrams

Using MATLAB software to read out the image given by the attachment and draw the image matrix, through the Sobel operator to find out the gradient of the digital elevation map S(x, y) , and set the gate value to 10.5, the data information 0-1 standardized after the updated image matrix, the reading results can be found in Figure 8.

From Figure 8 can find that the image has a large noise interference, using the median filter method to the image multiple noise processing, to get 5.9. In Figure 9, the image centre is the projection of the position of the Chang'e-3 on the lunar surface at the initial moment of the rough obstacle avoidance stage. Due to the gradient treatment, the denser the black spots in the image are, that is, the darker the colour is, and the flatter the region is.

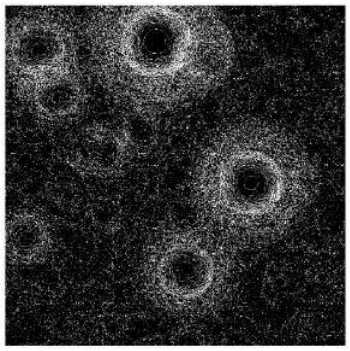

Figure 8: *Digital elevation chart of rough barrier avoidance segments.*

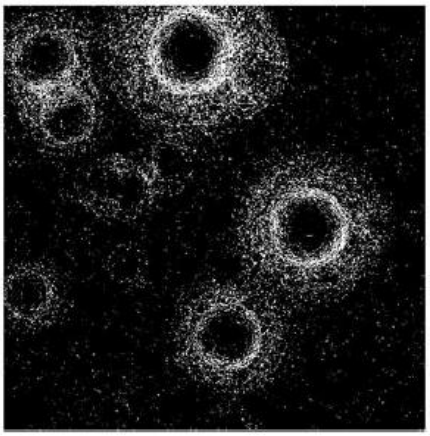

Figure 9: *Denoise Gradient.*

Solution of the optimal landing point of the rough barrier avoidance segment

The optimization target of optimal fuel consumption should also be regarded as the optimization target in the rough obstacle avoidance stage, because the centre point of the image is the projection of the position of the first moment of the rough obstacle avoidance stage, the optimization target of the optimal fuel consumption can be understood as the optimal landing point from the centre of the image. In the image centre for the selection of regional centre, select a pixel of 1800 × 1800 area, the area is divided into 9 × 9 grid areas, using MATLAB to solve the data matrix of each grid area, the data matrix of each area is combined and normalized, and the naturalization data matrix of 81 grid areas is obtained. It is easy to know that in this normalized image data matrix, the smaller the value indicates that the grid area is relatively flat [26]. Normalized image data for some grid areas is shown in (Table 2) below.

Table 2: *Normalized data information table for rouge barrier segment grid areas.*

Grid area number	3	4	5	6	7
3	0.00255100284362800	0.012896054724347	0.0144625680783822	0.00434118027775291	0.0012703744844633
4	0.0135984632015258	0.00910580637165461	0.00377658585622121	0.00201739226230231	0.00985286118551058
5	0.00635168724223166	0.00522938369699181	0.00137361691579969	0.00455118186137141	0.0307428547821836
6	0.00239264099368618	0.00129443599082878	0.000791809249709096	0.00749808932985396	0.0394217726887777
7	0.00278854561854073	0.000678201835620400	0.00246149397192176	0.00444445974510628	0.0203357271218767

As can be seen from the table above, the area (6,5) and (7,2) and other areas of the normalized value are relatively small, considering the lighting needs of Chang'e-3 working on the lunar surface and the need for flatness of the ground, the landing site cannot be in the crater. Since the optimal fuel consumption can be understood as the optimal distance to the centre of the image, the grid area closer to the centre point should be selected as the landing point [27]. Since there is only a very small horizontal directional displacement relative to the entire soft landing process during the coarse barrier avoidance phase, a more levelled area should be selected at similar distances.

The normalized data of Table 2 can be determined area (7,2) as the best landing area, the landing point centre is located in the regional centre, i.e. moving 44 pixels (44m) below the left, the above is north, the landing point can be used relative to the initial position of the rough barrier avoidance phase to move 44m west, combined with the obtained rough barrier initial position (unit: m) coordinate (380653.334, 1695.66). The position coordinates (380,609.334, 1692258.626) at the end of the rough barrier phase under the right-angle coordinate system of the moon's heart plane can be obtained.

Optimal motion trajectory and control strategy for coarse barrier avoidance segments

The initial state of the Chang'e-3 in the rough barrier phase can be regarded as the state of the end of the period of rapid adjustment, and the result of the solution of the rapid adjustment segment optimization model can be seen. The initial velocity of the coarse barrier segment is 0.0098 m/s and 0.1807 m/s on the right-angle coordinate system of the moon centre plane x-axis and the y-axis, and the mass of the Chang'e-3 is 1295.9kg. For the solution

Of the optimal track design and control strategy of the coarse barrier avoidance stage, the optimization target, the two-body dynamics model and the constraints are established in turn as follows:

Optimising goals

The optimization goal of the track design and control strategy of the Chang'e-3 in the rough barrier avoidance stage is still to have the lowest fuel consumption, that is,

$$\text{Min } Z = \int_{t_0}^{t_{f3}} \frac{\sqrt{u_x^2(t)+u_y^2(t)}}{v_e} dt. \quad (13)$$

Where in, t_{f3} is the end of the rough barrier phase, and other symbols are consistent with the general optimization model of the equation (4).

$$\begin{aligned} \frac{d^2x}{dt^2} &= \frac{GM_M}{x_3^2+y_3^2} sin \propto_3 (t) + \frac{u_{x3}(t)}{m_3(t)}, \\ \frac{d^2y}{dt^2} &= \frac{GM_M}{x_3^2+y_3^2} cos \propto_2 (t) + \frac{u_{y3}(t)}{m_3(t)}, \\ \frac{dm}{dt} &= \frac{\sqrt{u_{x3}^2(t)+u_{y3}^2(t)}}{v_e}, \\ u_3(t).cos\big(\alpha_3(t)-\theta_3(t)\big) &= u_{x_3}(t), \\ u_3(t).sin\big(\alpha_3(t)-\theta_3(t)\big) &= u_{x_3}(t), \end{aligned} \quad (14)$$

Among them, $\alpha_3(t)$ is the moon's gravity and the moon's centre plane right-angle coordinate system y axis angle, the main engine thrust direction and speed reverse angle of $\theta_3(t)$, the Chang'e-3 in the rough barrier section of the motion of $\alpha_3(t)$ and $\theta_3(t)$ will continue to change, its two-body dynamics model and the main deceleration segment is basically consistent.

Boundary constraints

The initial state of the rough barrier section during the soft landing process can be seen as its state at the end of the fast

adjustment phase, and the solution results and attachment information of the fast-adjusting segment optimization model can list the boundary constraints of the quality (unit: kg), position coordinates (unit: m) and flight speed (unit: m/s) in the rough barrier phase of the Chang'e-3.

$$m_3(t_0) = 1295.9, \frac{dx(t_0)}{dt} = 0.0098, \frac{dy(t_0)}{dt} = 0.1807,\ y_3(t_0) = 1736773, y_3(t_{f_3}) = 1734473, \frac{dx(t_{f_3})}{dt} 0, x_3(t_{f_3}) - x_3(t_0) = 44 \quad (15)$$

At this point, the joint up-type (9), (10), (11), to establish the track design and control strategy optimization model of the Chang'e-3 in the rapid adjustment stage. The model is also converted into differential iteration format, the optimal solution of the numerical optimization model of the rapid adjustment stage optimization model is solved when error allows, using the improved real-number coding genetic algorithm to find the optimal solution to the unknown parameters in $\theta_3(t)$ expression, to determine the optimal parameters and then replace them into the differential iteration format.

Solution and analysis of coarse barrier avoidance stage model

The rough barrier avoidance stage and the main deceleration stage are different from the need for horizontal displacement control, from the captured image to know that the spacecraft needs 44m horizontal displacement, while down to 1734473m, call the main deceleration stage model, assuming the thrust direction and speed inverse direction angle of $\theta(t)$ thrust size of $F(t)$. May set $\theta(t)$ and $F(t)$ to meet.

$$\begin{cases} \theta(t) = c_1 t^2 + c_2 t + c_3 \\ F(t) = c_4 t^2 + c_5 t + c_6 \end{cases}$$

Discrete of dynamic equation (14) is iteratively solved, and the above parameters are solved as

$$\begin{cases} \theta(t) = -9.287 \times 10^{-5} t^2 + 9.481 \times 10^{-5} t + 0.4778 \\ F(t) = F(t) = 0.1t^2 + 0.1t + 1430.32 \end{cases}$$

The resulting angle and thrust size are replaced with iterative model, and the solution of the time dispersion of each control parameter is obtained, and the specific parameters of the control strategy obtained through the constraints are shown in Figure 10. The horizontal velocity first increases, and then the thrust basically coincides with the angle in the vertical direction. In the rough obstacle avoidance phase of the movement trajectory into a straight line, in the end of the movement of violent deceleration. The rough obstacle avoidance stage takes 133s, with the horizontal velocity of -0.5412m/s, the vertical velocity of 0.0775m/s, and the final velocity of 0.5401m/s. The final height is 99.9990m, and the final horizontal displacement is 44.0047m. The mass of fuel consumed was 91.98kg, and the final mass was the Angle between thrust and vertical direction was 1.0455°.

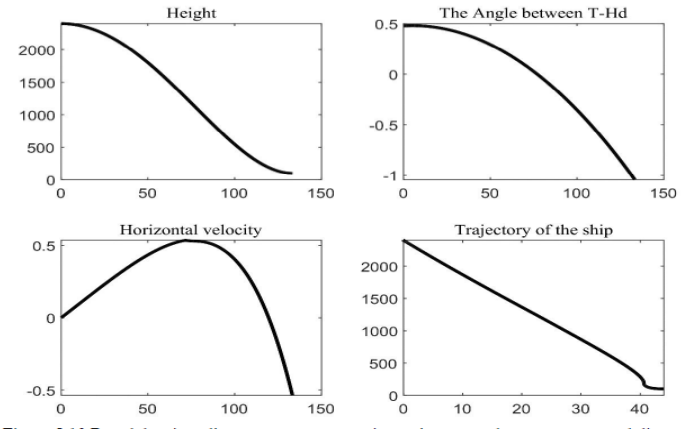

Figure 10: *Rough barrier adjustment segment motion trajectory and parameter control diagram.*

Establishment and solution of the model of the precision barrier avoidance segment

The role of the precision barrier avoidance phase of the soft landing process should be understood as further determining the optimal landing site over the lower lunar surface and determining the optimal control strategy for the main thrust engine to move the Chang'e-3 over the optimal landing site. The initial state of the fine obstacle avoidance stage can be understood as the end state of the rough obstacle avoidance stage. According to the solution results of the optimization model of the rough obstacle avoidance stage, it can be seen that Chang'e-3 is 99.9990m above the earth's surface, its flight speed is -0.5412m/s and 0.0775m/s on the x axis and y axis, and its final speed is 0.5401m/s. Its final mass is 1205.7kg.

Establishment and solution of the optimal landing point model of the precision barrier-avoidance segment

With coarse phase digital elevation map of obstacle avoidance are of a similar process for obstacle avoidance section digital elevation map, Sobel operator is used to calculate the gradient and the gradient information S(x, y) , median filtering method is used to many times to deal with the noise of the gradient map, through meshing the elevation graph corresponding to the demonising of gradient graph is divided into multiple regions, with fuel consumption optimal, the optimal flatness as the optimization goal to further determine the best landing site.

Image processing for digital elevation diagrams

Using MATLAB software to read out the image given by the attachment and draw the image matrix, through the Sobel operator to find out the gradient of the digital elevation map S(x, y) , with 14 for the gate value of data information 0-1 standardized after updating the image matrix, the matrix reading results see the following Figure 11, from Figure 11 can find that the image has a

large noise interference, using the medium filter method to make multiple noise processing of the image, to obtain Figure 12. In Figure 13, the denser the black spots of the image, the darker the colour, the more flat the area. The centre point of the image is a projection of the position of the lunar surface at the initial moment of the precision barrier-avoidance phase of the Chang'e-3.

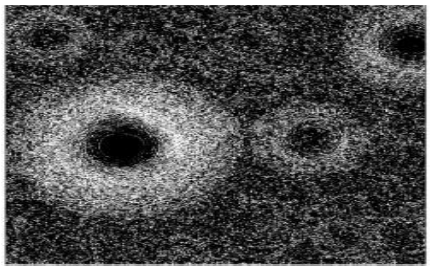

Figure 11: *Digital elevation chart of the precision barrier-avoidance segment.*

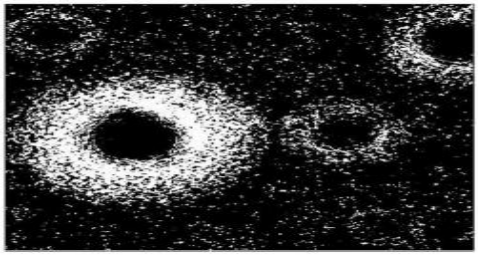

Figure 12: *Denoise Gradient.*

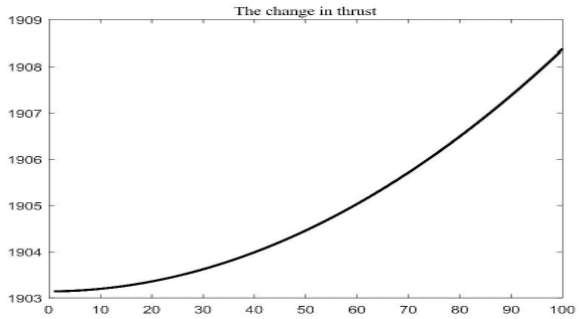

Figure 13: *Change of thrust with time.*

Solution of the optimal landing point of the precision barrier section

The Chang'e-3 should also optimize fuel consumption in the precision barrier-avoidance phase. Because the centre point of the image is the projection of the position of the first moment of the precision barrier-avoidance phase, the optimization target of the optimal fuel consumption can be understood as the optimal landing point from the centre of the image. In the image centre for the selection of regional centre, select a pixel of 1800 × 1800 area, the area is divided into 9 × 9 grid areas, using MATLAB to solve the data matrix of each grid area, the data matrix of each area is combined and normalized, and the naturalization data matrix of 81 grid areas is obtained. In this normalized image data matrix, a smaller value indicates that the grid area is relatively flat. Normalized image data for some grid areas is shown in (Table 3) below. As can be seen from the normalized data in table 3, the normalized value of region (6,3) is relatively small, but it is located to the left of the central point, that is, in the crater, where the sunlight is not enough, so it is not the optimal landing site. Can be found at the upper right of this centre point values are much smaller than the lower value, while smaller values (3, 6) area, but compared with the coarse obstacle avoidance, the essence of obstacle avoidance of falling distance is smaller, less time spent, to move a long distance, will consume more energy, the choice of probe landed close area as well, so the probe eventually fall to the ground area should be (4, 6), which need to be on the basis of the coarse obstacle avoidance to the northeast direction about 14 m (Figure 14).

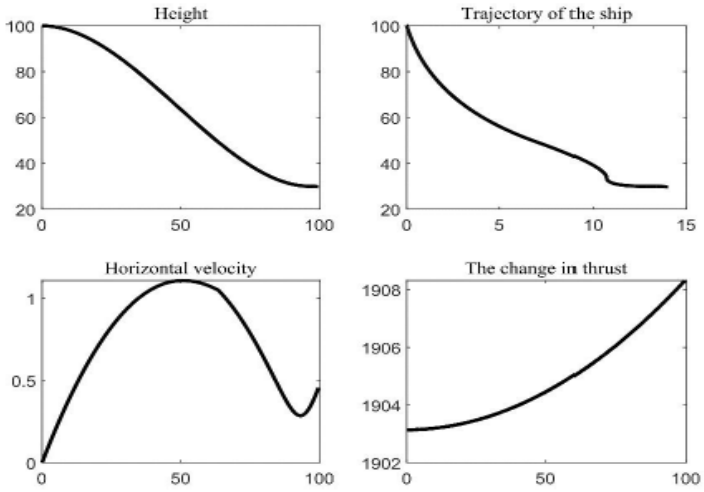

Figure 14: *Diagram of the motion trajectory and parameter control of the fine barrier adjustment segment.*

Table 3: *Normalized Data Information Table (partial) for the mesh area of the precision barrier avoidance segment.*

Grid area number	3	4	5	6	7
3	0.00998950	0.00818448 987039052	0.00348622 777122526	0.00196792 670450473	0.00267168 857234086

4	0.03986029 02366073	0.03793146 14136491	0.01956848 97139990	0.00264562 331797655	0.00263259 069079440
5	0.01253738 73492288	0.04186079 85090675	0.03971041 50240126	0.01479854 81653319	0.01252435 47220466
6	0	0.02084568 71778497	0.04261669 08856322	0.01327373 07850203	0.01369077 48548491
7	0.02278103 23143991	0.03439961 94472863	0.03392392 85551378	0.00529124 663595311	0.00368171 717895752

Optimal motion trajectory and control strategy for the precision barrier-avoidance segment

The Chang'e-3 in the pure phase of obstacle avoidance of the initial state can be considered as crude at the end of obstacle avoidance phase state. In fact, the essence of obstacle avoidance phase requires real-time image of the moon's surface are extracted and more elaborate obstacle avoidance adjustments, pure phase of the initial state of obstacle avoidance can be thought of as the hover state, at the end of this with coarse obstacle avoidance phase results [28]. According to the solution results of the optimization model for rough obstacle avoidance segment, the initial velocity of the fine obstacle avoidance segment is -0.5412m/s, 0.0775m/s, and the final mass is 1205.7kg in the x-axis and y-axis of the Cartesian coordinate system at the centre of the moon. In order to solve the optimal trajectory design and control strategy in the precise obstacle avoidance stage, the optimization objective, two-body dynamics model and constraint conditions are established as follows.

Optimising goals

The optimal goal of orbit design and control strategy of the Chang'e-3 in the precise obstacle avoidance stage is still to minimize fuel consumption, i.e

$$\text{Min } Z = \int_{t_0}^{t_{f4}} \frac{\sqrt{u_{x4}^2(t)+u_{y4}^2(t)}}{v_e} dt. \qquad (16)$$

Among them, t_{f4} is the end of the barrier-avoidance phase, other symbols and the general optimization model of the same meaning.

Two-body dynamics model

The Chang'e-3 is still only subject to engine thrust and the moon's gravitational pull in the precision barrier-avoidance phase.

$$\frac{d^2x}{dt^2} = \frac{GM_M}{x_4^2+y_4^2} sin \propto_4 (t) + \frac{u_{x4}(t)}{m_4(t)},$$

$$\frac{d^2y}{dt^2} = \frac{GM_M}{x_4^2+y_4^2} cos \propto_4 (t) + \frac{u_{y4}(t)}{m_4(t)},$$

$$\frac{dm}{dt} = \frac{\sqrt{u_{x4}^2(t)+u_{y4}^2(t)}}{v_e}, \qquad (17)$$

$$u_4(t).cos\big(\alpha_4(t)-\theta_4(t)\big) = u_{x_4}(t),$$

$$u_4(t).sin\big(\alpha_4(t)-\theta_4(t)\big) = u_{x_4}(t),$$

Among them, $\alpha_4(t)$ is the stage of the fine barrier-avoidance phase of the moon's gravity and the moon's centre plane right-angle coordinate system y-axis angle, the main engine thrust direction and speed of the reverse angle of $\theta_4(t)$ the Chang'e-3 in the process of the movement of the fine barrier-avoidance section $\alpha_4(t)$ and $\theta_4(t)$ will continue to change, its two-body dynamics model and coarse barrier avoidance section is basically the same.

Boundary constraints

The Chang'e-3 in a soft landing process essence of obstacle avoidance of the initial state can be regarded as the moment at the end of the coarse obstacle avoidance phase state, from coarse obstacle avoidance for solution of the optimization model with the attached information can be listed in the fine quality of obstacle avoidance phase change three (unit: kg), coordinates (unit: m) and speed (unit: m/s), the boundary constraint conditions are as follows The flight speed of the Chang'e-3 from the Earth's surface of the earth is 99.9990m on the x and y axes with a component of -0.5412m/s, 0.0775m/s, and a final speed of 0.5401m/s. The final mass is 1205.7kg

$$m_2(t_0) = 1205.7, \frac{dx_2(t_0)}{dt} = 0.5412, \frac{dy_2(t_0)}{dt} = -0.0075,$$

$$\sqrt{x_2^2(t_{f_2}) + y_2^2(t_{f_2})} = R + 30, \sqrt{\left(\frac{dx_2(t_{f2})}{dt}\right)^2 + \left(\frac{dy_2(t_{f2})}{dt}\right)^2} = 0 \qquad (18)$$

Among them, R is the radius of the moon, the upper type (16), (17), (18), the establishment of the orbit design and control strategy optimization model of the Chang'e-3 in the rough obstacle-avoiding stage. The model is also converted into differential iteration format, the optimal solution of the unknown parameters in $\theta_4(t)$ expression is sought by the improved real-number coding genetic algorithm, the optimal parameters are determined and replaced into the differential iteration format, and the numerical optimal solution of the coarse barrier-avoidance stage optimization model is solved under the condition of error.

Solution and analysis of the stage model of precision barrier avoidance

The horizontal displacement is different between the fine obstacle avoidance stage and the rough obstacle avoidance stage, and the descending height is much lower than that of the rough obstacle avoidance stage. As previously known, the horizontal displacement of 14m is required in the fine obstacle avoidance stage. Then, the discrete time iterative solution is used to obtain the variable force F in the fine obstacle avoidance stage by using the solution method of rough obstacle avoidance

$$F(t) = 5.1929 \times 10^{-4}t^2 + 3.9394 \times 10^{-4}t + 1903.14$$

Its change curve with time as shown in the figure below.

The angle $\theta(t)$ between thrust and vertical direction satisfies the following formula

$$\theta(t) = 1.0209 \times 10^{-4}t^2 - 8.0889 \times 10^{-4}t + 0.0561$$

It is substituted into the iterative discrete model to obtain the parameters of the optimal control strategy as shown in the figure below.

As the height decreases, the decreasing speed first increases and then decreases. The velocity first increases and then decreases to meet the requirement of zero velocity at the beginning and the end. The trajectory is basically an inverted parabola; the thrust increased from 1903.14N to 1908N, and the Angle between the thrust and the vertical direction was basically 0, that is, the thrust was basically vertical upward. The precision obstacle avoidance stage takes 97.8s, and the horizontal velocity is -0.1382m/s. The vertical velocity is 0.0712m/s, and the final velocity is 0.1554m/s. The final height is 29.9990m, and the final horizontal displacement is 14.0012m. The fuel mass consumed is 63.38kg, and the final mass is 1,140.5 kg. The Angle between thrust and the vertical direction is 0.9540°.

Establishment and solution of slow descent stage model

The initial state of the Chang'e-3 in the slow descent phase can be understood as the end state of the precision barrier-avoidance phase. According to the results of the solution of the optimization model of the fine barrier avoidance segment, the flight speed at the end of the precision barrier avoidance phase of the no. 3 is of -0.1382m/s, 0.0712m/s on the x, y axis, and the final mass is 1140.5kg. The effect of the slow descent phase should be understood to be to start slowly falling at a low speed value at 30m above the optimal landing point, so that the Chang'e-3 can hover over the optimal landing point at the end of the slow descent phase by hovering at 4m. For the solution of optimal track design and control strategy in the slow descent stage, the optimization target, the two-body dynamics model and the constraints are established in turn as follows:

Optimising goals

The optimization goal of the orbit design and control strategy of the Chang'e-3 in the slow descent stage is still to have the lowest fuel consumption, that is,

$$\text{Min } Z = \int_{t_0}^{t_{f5}} \frac{\sqrt{u_{x5}^2(t)+u_{y5}^2(t)}}{v_e} dt. \qquad (19)$$

Among them, t_{f5} is the end of the slow descent phase, and other symbols are consistent with the general optimization model of the equation (4).

Two-body dynamics model

The Chang'e-3 is still only subject to engine thrust and the moon's gravitational pull during the slow descent phase.

$$\begin{aligned}
\frac{d^2x_5}{dt^2} &= \frac{GM_M}{x_5^2+y_5^2} sin \propto_5 (t) + \frac{u_{x5}(t)}{m(t)}, \\
\frac{d^2y_5}{dt^2} &= \frac{GM_M}{x_5^2+y_5^2} cos \propto_5 (t) + \frac{u_{y5}(t)}{m(t)}, \\
\frac{dm}{dt} &= \frac{\sqrt{u_{x5}^2(t)+u_{y5}^2(t)}}{v_e}, \qquad (20) \\
u_5(t).cos\big(\alpha_5(t)-\theta_5(t)\big) &= u_{x_5}(t), \\
u_5(t).sin\big(\alpha_5(t)-\theta_5(t)\big) &= u_5(t),
\end{aligned}$$

Among them, $\alpha_5(t)$ is the moon's gravity and the moon's centre plane right-angle coordinate system y -axis angle, the main engine thrust direction and speed reverse angle is $\theta_5(t)$, the Chang'e-3 in the slow descent of the motion of $\alpha_5(t)$ and $\theta_5(t)$ will continue to change, its two-body dynamics model and the main deceleration segment is basically consistent.

Boundary constraints

The Change - 3 in a soft landing process slow down the initial state can be considered as the state of moments at the end of the pure phase of obstacle avoidance, the essence of obstacle avoidance for solution of the optimization model with the attachment information is listed in slow decline phase change three quality (unit: kg), coordinates (unit: m) and speed (unit: m/s), the boundary constraint conditions are as follows

$$\begin{aligned}
&m_2(t_0) = 1140.5, \frac{dx_2(t_0)}{dt} = 0.1382, \frac{dy_2(t_0)}{dt} = 0.0712, \\
&\sqrt{x_2^2(t_{f_2}) + y_2^2(t_{f_2})} = R + 4, \sqrt{\left(\frac{dx_2(t_{f2})}{dt}\right)^2 + \left(\frac{dy_2(t_{f2})}{dt}\right)^2} = 0
\end{aligned} \qquad (21)$$

So far, the joint up-type (19), (20), (21), to establish the Change-3 in the slow decline stage of the track design and control strategy optimization model. The model is also converted into differential iteration format, the optimal solution of the optimal solution of the differential decline stage optimization model is solved by using the improved real-number coding genetic algorithm to find the optimal solution to the unknown parameters in $\theta_5(t)$

expression to determine the optimal parameters and then replace them into the differential iteration format.

Solution and analysis of slow-down stage model

The slow descent phase is mainly to carry out altitude drop, the height of 29.990m down to 4m. At this time the thrust is basically equal to gravity, it may be said that the thrust size of the slow descent stage is variable force F, which meets the secondary three-way formula, iterative solution is obtained

$$F(t) = 9.5610 \times 10^{-4}t^2 + 7.6531 \times 10^{-4}t + 1816.54$$

Replace it into iterative model, use the genetic algorithm of double-precision real-number coding to obtain the time discrete value of the control parameters, and obtain the control strategy as Shown in Figure 15.

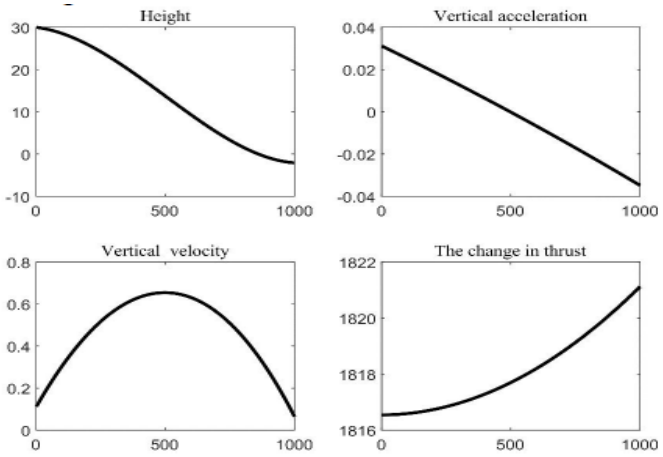

Figure 15: *A schematic diagram of the movement trajectory and parameter control of the slow descent adjustment section.*

The height drops from 29.990 m to 4.001m, accelerating first and then decelerating; the velocity first increases and then decreases in a symmetric form. The value of acceleration decreases from positive value to -0.036. The thrust increases gradually, and its size change value is 4 N. The slow descent stage takes 68.8s, with a horizontal velocity of 0m/s, a vertical velocity of 2.7077× $10^{-4}m/s$, and a final velocity of 2.7077× $10^{-4}m/s$. The final height is 4.0001m, and the final horizontal displacement is 0m. The fuel mass consumed is 42.57kg and the final mass is 1097.8kg [29].

Establishment and solution of free-fall stage model

Free fall refers to the movement of conventional objects, with zero initial velocity, called free-fall motion, only under the action of gravity. Free-fall motion is an ideal physical model. Free fall is the inertia trajectory of any object under the action of gravity, only gravity is the sole force, and it is the uniform acceleration motion with the initial speed of 0. It can be seen that the free fall phase does not consume fuel, at a horizontal speed of 0m/s, vertical direction speed is 2.7077× $10^{-4}m/s$ of the initial state of free fall. Its state of motion satisfies Newton's second law.

$$h = \frac{1}{2}gt^2$$

Where g is the moon's gravity acceleration, given by the following formula

$$g = \frac{GM}{R^2}$$

The gravity acceleration of the moon at this time was calculated to be 1.6256m/s^2, which was substituted into the height formula to obtain the free fall phase which took 2.2191s with a horizontal velocity of 0m/s and a final velocity of 3.6051m/s. The vertical velocity and vertical displacement are shown in the (Figure 16). The result is in line with the law of free fall motion, from the height of 4.0001 to 0 m, to reach the target location. During the motion, the moon's gravity worked hard, the spacecraft did not consume fuel, the final mass of 1097.8 kg.

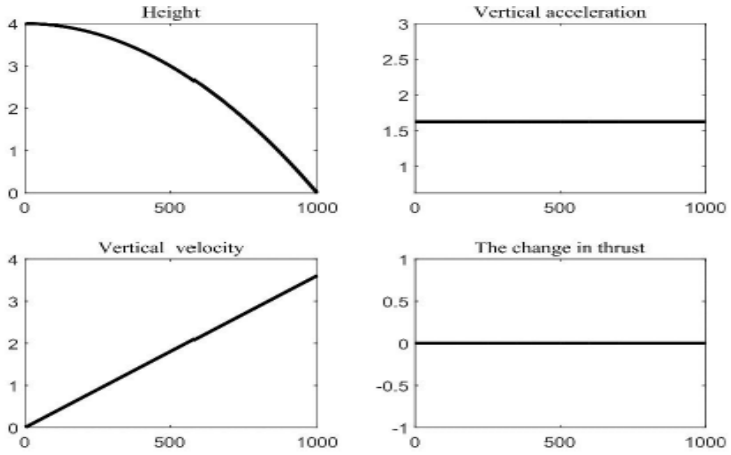

Figure 16: *Chart of motion trajectory and parameter control of free-fall adjustment segment.*

Error and Sensitivity Analysis

The numerical calculation method divides the non-negligent error into model error, observation error, truncation error and rounding error into four kinds, and the emphasis of the error analysis of different engineering problems is often different [30]. Sensitivity analysis of models is often divided into local sensitivity analysis and global sensitivity analysis [31]. In the problem of optimal orbit design and control strategy of soft landing on the Chang'e-3, it is necessary to design the motion trajectory to meet the basic requirements under the optimal condition of fuel consumption, and give the control strategy of important parameters, we should focus on analysing the system deviation of the key parameters of the model built by the soft landing process and give the global sensitivity analysis based on the sensitivity effect of the total order of each parameter as far as possible.

Solution and analysis of error propagation

In the two-body dynamics optimization model established for the soft landing process of the Chang'e-3, the functions of these key parameters, such as the flight time of the Chang'e-3 and the horizontal displacement of the horizontal displacement under the right-angle coordinate system of the moon's centre plane, also contain errors due to the system deviation such as the main engine thrust size, the near-moon point speed size, and the overall mass of the chang-3. The basic idea of error analysis is to find out the main engine thrust size, near-moon point speed, overall mass of the partial differential, the boundary constraints of each stage and other known data, such as the basic requirements of the differential expression to obtain a multi-equation equation, so as to determine the main error term affecting the target function.

For the general binary function $z = f(x, y)$, the absolute errors of the arguments x and y are δ_x and δ_y respectively, i.e.$|\Delta x| \leq \delta_x |\Delta y| \leq \delta_y$, and the error of the argument is [6].

$$|\Delta z| \approx |dz| = \left|\frac{\partial z}{\partial x}\Delta x + \frac{\partial z}{\partial y}\Delta y\right| \leq \left|\frac{\partial z}{\partial x}\right| . |\Delta x| + \left|\frac{\partial z}{\partial y}\right| . |\Delta y| \leq \left|\frac{\partial z}{\partial x}\right| \delta_x + \left|\frac{\partial z}{\partial y}\right| \delta_y$$

Thus the absolute error of z is about

$$\partial_z = \left|\frac{\partial z}{\partial x}\right| \delta_x + \left|\frac{\partial z}{\partial y}\right| \delta_y$$

So the relative error of z is about

$$\frac{\partial_z}{|z|} = \left|\frac{\partial z}{\partial x . z}\right| \delta_x + \left|\frac{\partial z}{\partial y . z}\right| \delta_y$$

Since the main deceleration stage is the longest time-consuming during the soft landing process of the Chang'e-3, the longest flight distance, the largest braking interval, that is, the stage with the largest fuel consumption, the error analysis for the model of this stage will be of great importance, and the global sensitivity analysis of the subsequent stage is similar, based on this, this section mainly makes the main deceleration stage based on the two-body dynamics of the fuel optimization model based on the error transmission of the key parameter system deviation calculation. In the optimization model established by the equation (4) based on two-body dynamics, the function of time t is

$$t_f = \left[1 - e^{\frac{v(t_f) - v(t)}{v_e}}\right] \frac{v_e . m_\Delta}{F} \quad (22)$$

The upper formula (22) is converted from $F = v_e . m$ conversion, where in, v_e is the ratio of the main deceleration engine, $. m_\Delta$ is the consumption quality of fuel in t_0 to t_f the pair (22) is obtained by partial differential

$$dt_f = \frac{\partial t_f}{\partial u}\partial u + \frac{\partial t_f}{\partial m_\Delta}\partial m_\Delta + \frac{\partial t_f}{\partial F}\partial F$$

Thus, the absolute error expression of the function of time t is as follows

$$\partial t_f = -\frac{v_e . m_\Delta}{v_e F} e^{\frac{u}{v_e}} \delta u + \left(1 - e^{\frac{u}{v_e}}\right) \frac{v_e}{F} \delta m_\Delta + \left(1 - e^{\frac{u}{v_e}}\right) \left(-\frac{v_e . m_\Delta}{F^2}\right) \delta F, u = v(t_f) - v(t_0) \quad (23)$$

Similarly, the function of horizontal displacement S is partially differential as follows

$$S = v(0)t_f - \frac{1}{2}\frac{1692.7}{t_f} . t_f^2 = \frac{1}{2} v(0)t_f \quad (24)$$

$$dS = \frac{1}{2} t_f dv + \frac{1}{2} v(0)dt \quad (25)$$

By the formula (25), the absolute error expression of the function of the available horizontal displacement S is

$$\delta S = \frac{1}{2} t_f \delta v + \frac{1}{2} v(0)\delta t \quad (26)$$

The function of velocity v is partially differential as follows

$$v = \sqrt{\frac{(1-e)GM}{k}}, e = \frac{c}{a}, k = a - c \quad (27)$$

$$dv = \frac{\partial v}{\partial k}dk + \frac{\partial v}{\partial e}de = -\frac{1}{2} \times \left(1 - e^{\frac{1}{2}}\right) \sqrt{GM} . k^{\frac{-3}{2}} dk - \frac{\sqrt{GM}}{2\sqrt{k(1-e)}} de \quad (28)$$

By the formula (28), the absolute error expression for the speed v is

$$\delta v = \frac{\delta v}{\delta k}\delta k + \frac{\delta v}{\delta e}\delta e = -\frac{1}{2} \times \left(1 - e^{\frac{1}{2}}\right) \sqrt{GM} . k^{\frac{-3}{2}} \delta k - \frac{\sqrt{GM}}{2\sqrt{k(1-e)}} \delta e \quad (29)$$

At this point, the relative error expression of the horizontal displacement S of changing of changing of changes such as junction (23), (26), (29) and ratio of punchv_e, lunar gravitational acceleration , and lunar mass M and so on is as follows.

$$\frac{\delta S}{S} = 0.4781\delta u + 0.4781\delta u + 0.4356\delta m + 0.4727\delta F + 0.4357\delta e + 0.4357\delta k \quad (30)$$

Where $u = v(t_f) - v(t_0)$the amount of speed is change, and $v(t_0) = 1.692.7m/s$ is the speed size at the near-moon point, and F is the speed. The main engine thrust size, e is the elliptical track eccentricity, and $k = a - c$ represents the difference between the length and half axis of the elliptical track. In the relative error expression (30) of horizontal displacement$S$, the error effect of each important parameter on the horizontal displacement of the Chang'e-3 can be expressed by the coefficient size of the corresponding error term.

Sobol solution and analysis of global sensitivity

In the sensitivity analysis of the optimal trajectory and control strategy model for the whole soft landing of the Chang'e-3, too few inputs are selected, which may greatly affect the analysis results and result in unreliable sensitivity analysis results. Selecting too many inputs may make the variance of the analysis results very large, resulting in unpractical sensitivity analysis. In addition, there is a certain interaction between the parameters of

the soft landing process. Even if the first-order sensitivity coefficient of a certain parameter is 0, there may be a non-zero higher-order sensitivity coefficient term. In fact, the global exploration sensitivity analysis method is more flexible to the second class of error than the local sensitivity analysis method [31]. Therefore, for the problem of optimal orbit design and key parameter control strategy of the soft landing process of Chang'e-3, the overall order sensitivity coefficient of the model should be analysed based on the total order effect of each parameter, similar to the error analysis, taking into account that the main deceleration stage is the stage with the most fuel consumption, and the global sensitivity analysis of the subsequent stage is similar, based on this, this section is mainly for the main deceleration stage based on the fuel optimization model based on the two-order dynamics of the global sensitivity analysis based on the Sobol overall effect. Sampling based on the range of arguments, which are generally sampled by Monte Carlo and a series of variants based on Monte Carlo sampling, this section uses Sobol sequence, which sets the number of samples sampled to N, the number of arguments is D, and generates a sample matrix of N * 2D (i.e. 4 rows and 6 columns). Set the first D column of the matrix as matrix A and the last D column as matrix B, and construct the matrix AB^i(i $=$ 1,2, … , D) of N*D, namely, replace the ith column of matrix A with the ith column of matrix A with the ith column of matrix B, construct the five matrices A 、 B、 AB^1、 $AB^2AB^3$and AB^3, get the input data of (D +2) * N group xi, and get D+2 N*D matrix YA, YB and Y_{ABi} (i = 1,2,…,D) .

Total effect exponential formula of method Sobol [31]

$$S_{Ti} = \frac{E_{Xi}\left(Var_{x\sim i}(Y|X_i)\right)}{Var(Y)} \qquad (31)$$

Among them

$$Var_{x\sim i}\left(E_{x\sim i}(Y|X_i)\right) \approx \frac{1}{N}\sum_{j=1}^{N} f(B)_j \cdot \left(f(AB^i)_j - f(A)_j\right)$$

$$E_{Xi}\left(Var_{x\sim i}(Y|X_i)\right) \approx \frac{1}{2N}\sum_{j=1}^{N}\left(f(A)_j - f(AB^i)_j\right)^2$$

$$Var(Y) = Var(Y_A + Y_B)$$

Substitute equations (22), (24) and (27) into equation (31), and use MATLAB to conduct Monte Carlo sampling to generate an N*2D (i.e., 4 rows and 6 columns) sample matrix. Then, the global sensitivity coefficient formula of horizontal displacement S in the main deceleration phase of Chang'e-3 based on the Sobol total order effect is obtained as follows:

$$\frac{\delta S}{s} = 38.2515\delta u + 35.3861\delta m + 37.8504\delta F + 35.3868\delta e + 35.3868\delta k \qquad (32)$$

In the formula (32) above, $u = v(t_i) - v(t_0)$ is the change in velocity, and $v(t_0) = 1692.7m/s$ is the velocity at the near lunar point; F is the main thrust of the engine; e is the eccentricity of the elliptical orbit; and $k = a - c$ is the difference between the length and half axis of the elliptical orbit. In the solution of global sensitivity coefficient formula, the horizontal displacement of the Chang'e-3 important parameters of the sensitivity of the size can be represented by the corresponding coefficient of sensitive factor of size, therefore, by type (32), the two body dynamics model has been established in the most sensitive factors for horizontal displacement S speed variation, and the key parameters of Chang'e-3 main reduction stage horizontal displacement of the sensitivity of S sort order from large to small is speed variation, and the size of the main force, eccentricity (tied for the difference between the short half long axis), the overall quality.

Competing Interest

We have no conflict of interests to disclose and the manuscript has been read and approved by all named authors.

Acknowledgement

This work was supported by the Philosophical and Social Sciences Research Project of Hubei Education Department (19Y049), and the Staring Research Foundation for the Ph.D. of Hubei University of Technology (BSQD2019054), Hubei Province, China.

References

1. Pengji W, Xun Z, Guangji Q. Modeling and simulation of lunar soft landing flight dynamics and guidance Control J. Science in China. 2009; 39: 521-527.
2. Rui J, Bing H. Research on landing control and software simulation of change-3 J. Microcomputer Applications. 2012; 28: 17-19.
3. Yao X, Xiaogang R, Ruoyan W. Optimal guidance method for fuel consumption of lunar surface soft landing based on three-dimensional model. China Process Control Conference.
4. Zhonggeng H, Jianping D. Comment on the design and control strategy of Change-3 soft landing track. Mathematical Modeling Appli. 2014; 31-38.
5. Jiarui P, Zhirong J, Lijun L. Design and control strategy of Change-3 soft landing track. Advances in Applied Mathematics. 2018; 7: 380-387.
6. Xiuzhi Z, Yumei Z, Cong Z. Change-3 soft landing track design and control strategy model. Sci Technol Innovation. 2018; 44-45.
7. Xiaoqun L, Wei L. Bear the mission of science and bravely shoulder the burden of exploring the moon. The important role of the Chinese Academy of Sciences in the task of Change-3. Bulletin of the Chinese Academy of Sci. 2014; 29: 124-128.
8. Honghua Z, Jun L, Xiangyu H. Change-3 autonomous obstacle avoidance soft landing control technology. Science in China: Technol Sci. 2014; 44: 559-568.
9. Jianping D, Zhonggeng H, DUJianping. Optimization model for design and control strategy of Change-3 soft landing track. Mathematical Modeling and Application. 2014.

10. Cuiping L, Yiming S, Xiaofeng Y. Change-3 soft landing track design and control optimization. Sci Technol Vision. 2015.
11. Qin Z. Chang'e-3 soft landing track design and control strategy. Time Report. 2016.
12. Lijia S, Wei L, Wenlian M. Research on Chang'e-3 Soft Landing Control. J Changchun University Sci and Technol. 2015; 63-67.
13. Yong H, Shengqi C, Peijia H. Orbit determination and lunar positioning of the Change-3 lunar probe. Chinese Science Bulletin. 2014; 59: 2268-2277.
14. Fanlu W, Jianjun L, Xin R. Research on the panoramic mosaic method of Change-3 panoramic camera image. Acta Optics Sinica. 2014; 34: 174-182.
15. Jie L. Multi-feature fusion particle filtering target tracking in complex scenes.
16. Danxiang J. Fish target detection and tracking method based on recognition sonar. 2018.
17. Xun Z, Guobiao C, Yingqiao X. Simulation analysis and experimental research of plume during soft landing of Change-3 lander. Science in China. 2014; 44: 344-352.
18. Yi L. Research on inversion and structural analysis of lunar shallow surface components based on change lunar exploration microwave data. Jilin University. 2014.
19. Yonghui Y, Hua LR. Design and control strategy of change-3 soft landing track. J Xian Aeronautical University. 2015.
20. Honghua Z, Yifeng G, Xiangyu H. Guidance, navigation and control of the power descent of Change-3 lander. Science in China. 2014; 44: 377-384.
21. Shengqi C, Yong H, Yezhi S. Strategy for determining the trajectory of the lunar landing segment of Change-3. J Aero craft Survey Control. 2014; 33: 236-243.
22. You H, Qi L, Jinhua L. Design and Control Strategy of Change-3 Soft Landing Track. Silicon Valley. 2014.
23. Xingwan Z, Jiaming Z. Change-3 soft landing track design and optimal control strategy. J Luoyang Institute Technol. 2015; 79-83.
24. Yu Z, Jianfeng C, Jianfeng D. Compensation and realization of the orbital dynamic model for continuous attitude control of the Change-3 probe. J Astronautics. 2015; 36: 489-495.
25. Yang J, Shaochuang L, Minglei L. Using landing image sequences to achieve high-precision positioning of the landing point of Change-3 system. Chinese Science Bulletin. 2014; 46-51.
26. Jianfeng C, Yu Z, Songjie H. Accurate positioning and accuracy analysis of Change-3 lander. J Wuhan University. 2016; 41: 274-278.
27. Peijia L, Yong H, Shengqi C. High-precision positioning of Chang'e-3 lander and patrol based on ground-based observations. Science Bulletin. 2014; 59: 3162-3173.
28. Xiangyu H, Honghua Z, Dayi W. Autonomous navigation and guidance technology for soft landing of Change-3 detector. J Deep Space Exploration. 2014; 52-59.
29. Jianzhong Y, Fuming Z, Jianfeng M. Design and verification of the landing buffer system of Chang'e-3 lander. Science in China. 2014; 440-449.
30. Dehua Z, Shen Y, Liu C. Three-dimensional laser scanner and analysis of the factors affecting its measurement error. Surveying Mapping Engi. 2005.
31. Saltelli A, Qiongli W. Global sensitivity analysis. Tsinghua University Press. 2018.